Available online at www.sciencedirect.com
SCIENCE DIRECT®

Journal of Sound and Vibration 294 (2006) 1051–1059

JOURNAL OF SOUND AND VIBRATION

www.elsevier.com/locate/jsvi

Free vibration analysis of plate using finite strip Fourier p-element

Li Yongqiang*

College of Science, Northeastern University, Shenyang 110004, China

Received 16 July 2004; received in revised form 17 March 2005; accepted 7 January 2006
Available online 17 February 2006

Abstract

A finite strip Fourier p-element for the in-plane vibration analysis of plate is presented. Trignometric functions are used as enriching functions instead of polynomials to avoid ill-conditioning problems. With the additional Fourier degrees of freedom (dofs) and reduce dimensions, the accuracy of the computed natural frequencies is greatly increased. Numerical examples show that convergence is very fast with respect to the number of trignometric terms. Comparison of natural frequencies calculated by the finite strip Fourier p-element, the Fourier p-element, the finite strip and the conventional finite elements is carried out. The results show that the finite strip Fourier p-element can obtain much higher accurate modes than the Fourier p-element, the finite strip and the conventional finite elements.
© 2006 Elsevier Ltd. All rights reserved.

1. Introduction

The finite element method achieves an approximate solution by subdividing the domain of interest into a number of smaller sub-domains, called finite elements, and then approximating the solution by using local, piecewise continuous polynomial functions within each element. The accuracy of the solution may be improved in two ways. The first is the h-version to refine the finite element mesh and the second is the p-version to increase the order of polynomial shape functions for a fixed mesh. Zienkiewicz and Taylor [1] concluded that, in general, p convergence is more rapid per degree of freedom (dof) introduced. Central to the hierarchical concept is the ability to enrich the polynomial content of selected elements within the mesh. Polynomial functions are well known to be ill-conditioned, e.g., the computer can hardly find the difference between x^{10} and x^{11} within $0<x<1$. West et al. [2] showed recently that, by reference to an appropriate family of K-orthogonal polynomials, numerical rounding errors associated with floating point arithmetic prescribe the maximum available degree of polynomial enrichment. The principal source of these errors can be traced to the widely ranged coefficients that define a given K-orthogonal polynomial. In a p-version finite element method, the trignometric functions are more effective in predicting the medium- and high-frequency modes than polynomials both in precision and in avoiding the ill-conditioning problems. The Fourier-p version elements are popular for the dynamic problems. Leung and Chan [3] gave the trignometric shape functions for

*Tel.: +86 2483684686.
E-mail address: lyq525@sohu.com.

0022-460X/$ - see front matter © 2006 Elsevier Ltd. All rights reserved.
doi:10.1016/j.jsv.2006.01.003

the axial vibration analysis of a two-node bar. Leung et al. [4] adopted trapezoidal Fourier p-element for the in-plane vibration analysis of two-dimensional elastic solids.

Cheung [5] proposed the finite strip method for structural analysis of prismatic domain problems and in contrast to discretize all domains as commonly carried out in FEM, only the transverse cross section is discretized. However, along the longitudinal coordinate, the functions and their differential are still continuous and smooth. Thus, the method is regarded as a semi-analytical method. The method may be reduced from three dimensions to two dimensions and two dimensions to one dimension, so it can save more time and makes the calculation results more accurate.

In this paper, we combine the finite strip method with the Fourier p-element method, to calculate the frequencies of plate.

2. Formulation

2.1. Shape function

The plate is imagined to be separated into a small number of strips, each strip having a constant thickness of its own (Fig. 1). Considering a typical strip defined by the sides i and j, it can be seen that a function

$$w = \sum N_m^e \delta_m^e, \tag{1}$$

where N_m^e is the shape function satisfies the boundary conditions, and $\delta_m^e = \{ w_{im} \quad \theta_{im} \quad w_{jm} \quad \theta_{jm} \quad w_p \}^{\mathrm{T}}$, $p = 1, 2, \ldots$ is the vector of nodal displacement for finite strip Fourier p-element. w_p represent internal displacement and are to be eliminated before assembling element matrix. It will be noticed that if the function w is defined for all the strips in the region, no discontinuities in its value and its slopes will occur along the imaginary boundary lines. Leung et al. [3] adopted the Fourier-enriched shape functions $f_i(\zeta) = [1 - \zeta, \zeta, \sin(p\pi\zeta)]$, $(p = 1, 2, \ldots)$ to analyze the axial vibration of a two-node bar. The sine functions represent internal dofs. When considering the bending of a plate, the appropriate shape functions of the finite strip Fourier p-element method are

$$\mathbf{N}_m^e = Y_m(y)\left[1 - \frac{3x^2}{a^2} + \frac{2x^3}{a^3},\ x - \frac{2x^2}{a} + \frac{x^3}{a^2},\ \frac{3x^2}{a^2} - \frac{2x^3}{a^3},\ \frac{x^3}{a^2} - \frac{x^2}{a},\ \frac{x}{a}\left(1 - \frac{x}{a}\right)\sin p\pi\frac{x}{a}\right] \quad (p = 1, 2, \ldots), \tag{2}$$

where $Y_m(y)$ is a series to satisfy the boundary conditions. Since the in-plane free vibration of plate is a truly two-dimensional problem, the shape functions N_m^e may reduce from two dimensions to one dimension to the in-plane free vibration of plate. For two opposite edges simplify or clamped supported boundary conditions, $Y_m(y)$ is

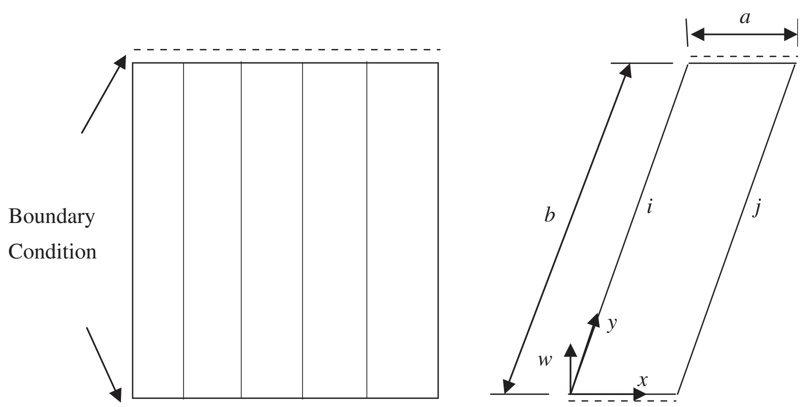

Fig. 1. A typical strip and an arbitrary problem.

(a) two opposite edges simplify supported,

$$Y_m(y) = \sin\frac{\mu_m y}{b},\ \ \mu_m = m\pi,\ \ m = 1, 2, \ldots, \infty \tag{3a}$$

(b) two opposite edges clamped supported

$$Y_m(y) = \sin\frac{\mu_m y}{b} - \sinh\frac{\mu_m y}{b} - \frac{\sin\mu_m - \sinh\mu_m}{\cos\mu_m - \cosh\mu_m}\left(\cos\frac{\mu_m y}{b} - \cosh\frac{\mu_m y}{b}\right), \tag{3b}$$

$$\mu_m = 4.730,\ 7.8532,\ 10.9960, \ldots, \frac{2m+1}{2}\pi,\ \ m = 1, 2, \ldots, \infty.$$

For the other boundary conditions, $Y_m(y)$ were given in Ref. [5].

2.2. Stiffness matrix and mass matrix

The strains of the plate strip are given by [6]

$$\boldsymbol{\varepsilon} = -z\left\{\frac{\partial^2 w}{\partial x^2},\quad \frac{\partial^2 w}{\partial y^2},\quad 2\frac{\partial^2 w}{\partial x \partial y}\right\}^{\mathrm{T}}. \tag{4}$$

Substituting Eq. (4) into the strain equations (4), as

$$\boldsymbol{\varepsilon} = \sum \mathbf{B}_m^e \delta_m^e, \tag{5}$$

where $\mathbf{B}_m^e$ is the strain matrix of the element. For the harmonic vibration of the plane problems, the stiffness matrix and the mass matrix of the element are obtained by applying the principle of minimum potential energy and the Hamilton's principle, respectively,

$$\mathbf{K}_m^e = \int_V \mathbf{B}_m^{e\,\mathrm{T}} \mathbf{D} \mathbf{B}_m^e \,\mathrm{d}V = \int_{-h/2}^{h/2}\int_0^b\int_0^a \mathbf{B}_m^{e\,\mathrm{T}} \mathbf{D} \mathbf{B}_m^e \,\mathrm{d}x\,\mathrm{d}y\,\mathrm{d}z, \tag{6}$$

$$\mathbf{M}_m^e = \int_V \rho \mathbf{N}_m^{e\,\mathrm{T}} \mathbf{N}_m^e \,\mathrm{d}V = \rho h \int_0^b\int_0^a \mathbf{N}_m^{e\,\mathrm{T}} \mathbf{N}_m^e \,\mathrm{d}x\,\mathrm{d}y. \tag{7}$$

For a plane stress problem, the rigidity matrix is

$$\mathbf{D} = D_0 \begin{bmatrix} 1 & \mu & 0 \\ \mu & 1 & 0 \\ 0 & 0 & (1-\mu)/2 \end{bmatrix}, \tag{8}$$

where $D_0 = E/(1-\mu^2)$, with E the Young's modulus, ρ the density, h the thickness of the element and μ the Possion's ratio.

The coefficients of the stiffness matrix and the mass matrix are given in Appendix A.

2.3. Free vibration analysis of structures

For different boundary conditions, $Y_m(y)$ concrete expression is substituted into the stiffness matrix and the mass matrix, and the stiffness matrix and the mass matrix of the element is calculated. The stiffness matrix and the mass matrix thus obtained can be stored in two individual files. These files are later used to compute the natural frequencies of the plane problems.

Before assembling the elements, the internal dofs and the dofs on some edges and at corner nodes not adjacent to other elements can be condensed by exact dynamic condensation [7]. The assembling is carried out by ensuring that the directions of the common edges are compactable between two adjacent elements. Then, for free vibrations, one has

$$[\mathbf{K} - \lambda\mathbf{M}]\mathbf{u} = 0, \tag{9}$$

where $\mathbf{K}$ is the global stiffness matrix of the structure, $\mathbf{M}$ is the global mass matrix of the structure, $\mathbf{u}$ is the eigenvector in terms of the master dofs of the structure, and $\lambda = \omega^2$ is the eigenvalue where ω is the natural frequency of the structure.

3. Numerical examples

To simplify the computation, the trignometric term p is given the same value as q in this paper. The following several cases of in-plane vibration are used to examine the performance of the new finite strip Fourier p-element.

3.1. Free vibration of square plates with two opposite edges simplify supported

To study the accuracy of the present elements, a square elastic plate with two opposite edges simplify supported is studied. The first six modes of $m = 1$ for a square plate of side b with various boundary conditions using five sine terms were computed and are tabulated in Table 1. The six boundary conditions are SSSS, SCSC, SFSF, SCSS, SFSS and SFSC. The non-dimensional frequency factor for the plate is λ, where $\lambda^2 = \omega a^2\sqrt{\rho h/D}$, $D = Eh^3/[12(1-v^2)]$ its flexural, h is the plate thickness, and Poisson's ratio $v = 0.3$. The results computed by ten finite strip Fourier p-elements with $p = q = 5$ are compared with the computed results of Fourier p-element method with $p = q = 5$ and 10×10 mesh, the computed results of finite strip method with a mesh of 10×1, the computed results of Q4 elements with a mesh of 10×10 and the exacts in Refs. [8,9] in Table 1. It can be found that the present method can obtain very high accurate frequencies of the plate.

Table 2 gives the convergence study of the first 8 natural frequency parameters of a square SSSS plate by means of a different number of sine terms and compares them to the exact solution. It is shown that the computed results of the present method with $p = q = 5$ produces extremely good results.

3.2. Free vibration of plates with two opposite edges clamped supported

An elastic plate of $b/a = 0.4$ with two opposite edges clamped supported is studied. The first five modes of $m = 1$ using five sine terms were computed and are tabulated in Table 3. The five boundary conditions are, respectively, CCCC, CCCS, CCCF, CSCF, and CFCF. The results computed by ten finite strip Fourier p-elements with $p = q = 5$ are compared with the exacts in Ref. [9] in Table 3. It can be found that the present method can obtain very high accurate frequencies of the plate.

3.3. Free vibration of disc

This example is the vibration analysis of a disc with inner radius clamped supported and outer radius free supported. The parameters of the disc are inner radius $r = 0.05\,\mathrm{m}$, outer radius $R = 0.5\,\mathrm{m}$, $E = 196 \times 10^9\,\mathrm{N/m^2}$, $\rho = 7800\,\mathrm{kg/m^3}$ and $\mu = 0.3$ (Fig. 2). This disc vibration problem is derived from the rectangular plate vibration problem by replacing x by $r - r_i$, y by θ and a by $r_j - r_i$ in Eq. (2), then $Y_m(\theta) = \cos m\theta$. The strains of the disc are given by

$$\varepsilon = -z\left\{\frac{\partial^2 w}{\partial r^2},\quad \frac{1}{r}\left(\frac{1}{r}\frac{\partial^2 w}{\partial \theta^2} + \frac{\partial w}{\partial \theta}\right),\quad \frac{2}{r}\left(\frac{\partial^2 w}{\partial r\partial\theta} - \frac{1}{r}\frac{\partial w}{\partial \theta}\right)\right\}^{\mathrm{T}}. \tag{10}$$

Table 1
Comparison of the frequency parameters λ^2 for square plates with two opposite edges simplify supported ($m = 1$)

Mode case		1	2	3	4	5	6
SSSS	Present	19.7392	49.3482	98.6967	167.7849	256.6000	365.0908
	Fourier-p 10×10	19.7386	49.3475	98.6969	167.7856	256.6010	365.0950
	Finite strip 10×1	19.7387	49.3471	98.6969	167.7854	256.6007	365.0969
	Q4 10×10	19.7276	49.3515	98.7390	168.0306	257.5496	365.6325
	Gorman	19.7392	49.3480	98.6960	167.7833	256.6097	365.1754
	Leissa	19.7392	49.3480	98.6960	167.7833	—	—
SCSC	Present	28.9509	69.3269	129.0958	208.3917	307.3159	425.9142
	Fourier-p 10×10	28.9513	69.3279	129.0943	208.3814	307.3286	425.9896
	Finite strip 10×1	28.9512	69.3283	129.0932	208.3819	307.3311	425.9413
	Q4 10×10	28.9318	69.3621	129.2091	208.9031	308.9896	427.3189
	Gorman	28.9509	69.3270	129.0955	208.4036	307.3487	425.8954
	Leissa	28.9509	69.3270	129.0955	—	—	—
SFSF	Present	9.6312	16.1349	36.7275	75.3025	133.8221	212.5878
	Fourier-p 10×10	9.6096	16.0807	36.6991	75.2396	133.6734	212.0865
	Finite strip 10×1	9.6294	16.1013	36.7178	75.2527	133.7942	212.3835
	Q4 10×10	9.5695	15.9715	36.0969	74.7419	132.4663	211.8841
	Gorman	9.6314	16.1348	36.7256	75.2834	133.9131	212.4935
	Leissa	9.6314	16.1348	36.7256	75.2834	—	—
SCSS	Present	23.6466	58.6460	113.2296	187.4166	282.2865	398.9184
	Fourier-p 10×10	23.6495	58.6479	113.2132	187.5366	281.7221	397.9603
	Finite strip 10×1	23.6484	58.6470	113.2202	187.4426	282.1355	398.5386
	Q4 10×10	23.6584	58.8486	112.6058	186.6445	280.5376	395.9961
	Gorman	23.6463	58.6464	113.2281	187.3263	282.3865	398.8813
	Leissa	23.6463	58.6464	113.2281	—	—	—
SFSS	Present	11.6846	27.7569	61.8699	115.7597	189.7462	284.1469
	Fourier-p 10×10	11.7636	27.9837	62.1885	116.8337	190.8492	285.8261
	Finite strip 10×1	11.7262	27.7832	61.9730	116.2005	190.0343	285.0853
	Q4 10×10	11.8211	28.2835	63.2016	117.4861	192.3689	288.0412
	Gorman	11.6845	27.7563	61.8606	115.6857	189.5246	284.4367
	Leissa	11.6845	27.7563	61.8606	115.6857	—	—
SFSC	Present	12.6874	33.0654	72.4047	131.4744	210.7581	310.4609
	Fourier-p 10×10	12.7092	32.5754	72.4449	132.1688	209.8969	309.0518
	Finite strip 10×1	12.6891	32.9726	72.1954	131.9554	210.0636	309.7426
	Q4 10×10	12.7590	31.6712	71.1785	129.9998	208.4291	308.3087
	Gorman	12.6874	33.0651	72.3976	131.4287	210.9711	310.2634
	Leissa	12.6874	33.0651	72.3976	131.4287	—	—

Table 2
Comparison of the frequency parameters λ^2 for square plates with fully simplify supported ($m = 1$)

Mode case		1	2	3	4	5	6	7	8
Present	$p = q = 1$	19.7374	49.3523	98.7032	167.7968	256.5581	364.9831	493.2628	641.2265
	$p = q = 2$	19.7379	49.3510	98.7014	167.7913	256.5779	365.0614	493.2912	641.3257
	$p = q = 3$	19.7386	49.3498	98.6991	167.7885	256.5840	365.0610	493.3250	641.3734
	$p = q = 4$	19.7390	49.3489	98.6981	167.7862	256.5968	365.0473	493.3383	641.4046
	$p = q = 5$	19.7392	49.3482	98.6967	167.7849	256.6000	365.0908	493.3476	641.4078
	$p = q = 6$	19.7392	49.3481	98.6963	167.7846	256.6013	365.0924	493.3743	641.4179
Exact		19.7392	49.3480	98.6960	167.7833	256.6097	365.1754	493.4802	641.5243

Table 3
Comparison of the frequency parameters λ^2 for a plate of $b/a = 0.4$ with two opposite edges clamped supported ($m = 1$, $v = 0.3$)

Mode case		1	2	3	4	5
CCCC	Present	23.646	27.810	35.427	46.619	61.463
	Leissa	23.648	27.817	35.446	46.702	61.554
CCCS	Present	23.439	27.016	33.781	44.047	57.914
	Leissa	23.440	27.022	33.799	44.131	58.034
CCCF	Present	22.578	24.619	29.234	37.133	48.197
	Leissa	22.577	24.623	29.244	37.059	48.283
CSCF	Present	22.542	24.285	28.293	35.258	45.591
	Leissa	22.544	24.296	28.341	35.345	45.710
CFCF	Present	22.347	23.078	25.615	30.571	38.585
	Leissa	22.346	23.086	25.666	30.633	38.687

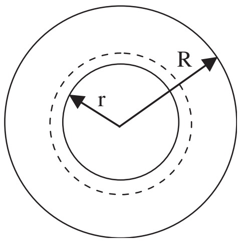

Fig. 2. A disc with inner radius clamped supported and outer radius free supported.

Table 4
Comparison of the frequencies λ for a disc with inner radius clamped supported and outer radius free supported ($p = q = 5$)

Numbers of nodal diameter	Numbers of nodal circle	Present (Hz)	Exact solution (Hz)	Error (%)
1	1	33.6068	33.6092	0.007
	2	267.2024	267.2022	0.0001
	3	746.2017	745.9713	0.0309
2	1	54.2807	54.2538	0.0496
	2	356.0836	355.9007	0.0514
	3	866.1829	865.99	0.0223
3	1	120.1101	120.006	0.0867
	2	511.7174	511.465	0.0493
	3	1083.4863	1083.2962	0.0175
4	1	210.3464	210.2548	0.0435
	2	706.2521	706.0	0.0358
	3	1364.5754	1363.49	0.0795

The frequencies of the disc using ten finite strip Fourier p-elements are computed and compared with exact solutions [10] in Table 4. The computed results show that the finite strip Fourier p-element can obtain the very accurate results with a simple mesh and a few trignometric terms.

4. Conclusions

A finite strip Fourier p-element method for the vibration analysis of plate is presented. For in-plane vibration problems, the present finite strip Fourier p-element is a better choice to obtain solutions with high accuracy.

For the in-plane vibrations of square plates with two opposite edges simplify supported, comparison with the results computed by the finite strip Fourier p-elements, the Fourier p-elements, the finite strip method and the traditional finite elements was carried out to examine the effectiveness. The results showed that the finite strip Fourier p-element was more accurate in predicting the natural modes than the Fourier p-elements, the finite strip method and the traditional finite elements. The eight lowest modes of an elastic square plates with fully simplify supported were analyzed with different number of Fourier terms. The computed results using five Fourier terms were in good agreement with the exact solutions.

In this way, a disc was analyzed by the finite strip Fourier p-elements and the results were compared with exact solutions. The computed results show that the finite strip Fourier p-element can give the very accurate results with a simple mesh and a few trignometric terms.

Acknowledgments

The author is very grateful to Bin Zhu of City University of Hong Kong for supporting this work.

Appendix A. The stiffness matrix and the mass matrix

$$k_{1,1} = k_{3,3} = \frac{eh^3}{420(1-\mu^2)a^3}\int_0^b \left\{13a^4\ddot{Y}_m^2 + 420\,Y_m^2 + 84a^2\left[\dot{Y}_m^2(1-\mu) - \ddot{Y}_m Y_m\mu\right]\right\}\mathrm{d}y,$$

$$k_{1,2} = k_{2,1} = -k_{3,4} = -k_{4,3} = \frac{eh^3}{2520(1-\mu^2)a^2}\int_0^b \left[11a^4\ddot{Y}_m^2 + 1260\,Y_m^2 + 42a^2\dot{Y}_m^2(1-\mu) - 252\,\ddot{Y}_m Y_m\mu\right]\mathrm{d}y,$$

$$k_{1,3} = k_{3,1} = \frac{eh^3}{280(1-\mu^2)a^3}\int_0^b \left\{3a^4\ddot{Y}_m^2 - 280\,Y_m^2 + 56a^2\left[\ddot{Y}_m Y_m\mu - \dot{Y}_m^2(1-\mu)\right]\right\}\mathrm{d}y,$$

$$k_{1,4} = k_{4,1} = -k_{2,3} = -k_{3,2} = \frac{eh^3}{5040(1-\mu^2)a^2}\int_0^b \left[-13a^4\ddot{Y}_m^2 + 2520\,Y_m^2 + 84a^2\dot{Y}_m^2(1-\mu) - 84\,\ddot{Y}_m Y_m\mu\right]\mathrm{d}y,$$

$$k_{2,2} = k_{4,4} = \frac{eh^3}{1260(1-\mu^2)a}\int_0^b \left\{a^4\ddot{Y}_m^2 + 420\,Y_m^2 + 28a^2\left[\dot{Y}_m^2(1-\mu) - \ddot{Y}_m Y_m\mu\right]\right\}\mathrm{d}y,$$

$$k_{2,4} = k_{4,2} = \frac{eh^3}{5040(1-\mu^2)a}\int_0^b \left\{-3a^4\ddot{Y}_m^2 + 840\,Y_m^2 - 28a^2\left[\dot{Y}_m^2(1-\mu) - \ddot{Y}_m Y_m\mu\right]\right\}\mathrm{d}y,$$

$$\begin{aligned} k_{1,4+p} = k_{4+p,1} = {} & \frac{eh^3}{6(1-\mu^2)ap^5\pi^5}\int_0^b \left\{60a^2\ddot{Y}_m^2 + p^2\pi^2\left[36\,\dot{Y}_m^2(1-\mu) + \ddot{Y}_m(a^2\ddot{Y}_m - 36\,Y_m\mu)\right]\right. \\ & \left. +12(-1)^p\left[5a^2\ddot{Y}_m^2 + 3p^2\pi^2\dot{Y}_m^2(1-\mu) - 3p^2\pi^2\ddot{Y}_m Y_m\mu\right]\right\}\mathrm{d}y, \end{aligned}$$

$$\begin{aligned} k_{2,4+p} = k_{4+p,2} = {} & -\frac{eh^3}{6(1-\mu^2)p^5\pi^5}\int_0^b \left\{-36a^2\ddot{Y}_m^2 + p^2\pi^2\left[20\,\dot{Y}_m^2(1-\mu) + \ddot{Y}_m(a^2\ddot{Y}_m + 36\,Y_m\mu)\right]\right. \\ & \left. +8(-1)^p\left[-3a^2\ddot{Y}_m^2 - 2p^2\pi^2\dot{Y}_m^2(1-\mu) + 2p^2\pi^2\ddot{Y}_m Y_m\mu\right]\right\}\mathrm{d}y, \end{aligned}$$

$$k_{3,4+p} = k_{4+p,3} = -\frac{eh^3}{6(1-\mu^2)ap^5\pi^5}\int_0^b \Big\{60a^2\ddot{Y}_m^2 + 36p^2\pi^2\Big[\dot{Y}_m^2(1-\mu) - \ddot{Y}_m Y_m\mu\Big]$$
$$+(-1)^p\Big[60a^2\ddot{Y}_m^2 + 36p^2\pi^2\dot{Y}_m^2(1-\mu) + p^2\pi^2\ddot{Y}_m(a^2\ddot{Y}_m - 36Y_m\mu)\Big]\Big\}\mathrm{d}y,$$

$$k_{4,4+p} = k_{4+p,4} = -\frac{eh^3}{6(1-\mu^2)p^5\pi^5}\int_0^b \Big\{-24a^2\ddot{Y}_m^2 - 6p^2\pi^2\Big[\dot{Y}_m^2(1-\mu) - \ddot{Y}_m Y_m\mu\Big] + (-1)^p\Big[-36a^2\ddot{Y}_m^2$$
$$-20p^2\pi^2\dot{Y}_m^2(1-\mu) + p^2\pi^2\ddot{Y}_m\big(a^2\ddot{Y}_m + 20Y_m\mu\big)\Big]\Big\}\mathrm{d}y,$$

$$k_{4+p,4+q} = k_{4+p,4+q} = -\frac{4pq\lfloor 1+(-1)^{p+q}\rfloor eh^3}{3(1-\mu^2)a^3(p^2-q^2)^4\pi^4}\int_0^b \Big\{3p^2q^2\pi^4 Y_m^2(p^2+q^2) + 3a^4\ddot{Y}_m^2(p^2+q^2)$$
$$+2a^2\pi^2(p^4+4p^2q^2+q^4)\Big[\dot{Y}_m^2(1-\mu) - \ddot{Y}_m Y_m\mu\Big]\Big\}\mathrm{d}y, \quad p \neq q,$$

$$k_{4+p,4+p} = \frac{eh^3}{720(1-\mu^2)a^3p^4\pi^4}\int_0^b \Big\{a^4\ddot{Y}_m^2[45+p^4\pi^4] + p^4\pi^4 Y_m^2(45+60p^2\pi^2+p^4\pi^4)$$
$$+2ap^2\pi^2(-15+10p^2\pi^2+p^4\pi^4)\Big[\dot{Y}_m^2(1-\mu) - \ddot{Y}_m Y_m\mu\Big]\Big\}\mathrm{d}y,$$

$$m_{1,1} = m_{3,3} = \rho h\frac{13a}{35}\int_0^b Y_m^2\,\mathrm{d}y, \quad m_{2,2} = m_{4,4} = \rho h\frac{a^3}{105}\int_0^b Y_m^2\,\mathrm{d}y,$$

$$m_{1,2} = m_{2,1} = -m_{3,4} = -m_{4,3} = \rho h\frac{11a^2}{210}\int_0^b Y_m^2\,\mathrm{d}y, \quad m_{1,3} = m_{3,1} = \rho h\frac{9a}{70}\int_0^b Y_m^2\,\mathrm{d}y,$$

$$m_{1,4} = m_{4,1} = -m_{2,3} = -m_{3,2} = -\rho h\frac{13a^2}{420}\int_0^b Y_m^2\,\mathrm{d}y, \quad m_{2,4} = m_{4,2} = -\rho h\frac{a^3}{420}\int_0^b Y_m^2\,\mathrm{d}y,$$

$$m_{1,4+p} = m_{4+p,1} = \rho h\frac{2a[60+\pi^2p^2+60(-1)^p]}{\pi^5p^5}\int_0^b Y_m^2\,\mathrm{d}y,$$

$$m_{2,4+p} = m_{4+p,2} = \rho h\frac{2a^2[36-\pi^2p^2+60(-1)^p]}{\pi^5p^5}\int_0^b Y_m^2\,\mathrm{d}y,$$

$$m_{4,4+p} = m_{4+p,4} = -\rho h\frac{2a^2[-24+(-36+\pi^2p^2)(-1)^p]}{\pi^5p^5}\int_0^b Y_m^2\,\mathrm{d}y,$$

$$m_{4+p,4+q} = m_{4+q,4+p} = -\rho h\frac{48apq(p^2+q^2)[1+(-1)^p]}{\pi^4(p^2-q^2)^4}\int_0^b Y_m^2\,\mathrm{d}y, \quad p \neq q,$$

$$m_{4+p,4+p} = -\rho h\frac{a}{60}\left(1+\frac{45}{p^4\pi^4}\right)\int_0^b Y_m^2\,\mathrm{d}y,$$

where $p, q = 1, 2, \ldots$.

References

[1] O.C. Zienkiewicz, R.L. Taylor, *The Finite Element Method*, vol. 1, fourth ed., McGraw-Hill, New York, 1989.

[2] L.J. West, N.S. Bardell, J.M. Dundon, P.M. Loasby, Some limitations associated with the use of K-orthogonal polynomials in hierarchical versions of the finite element method, *Proceedings of the Fifth International Conference on Recent Advances Structural Dynamics, Southampton* 1 (1997) 217–227.

[3] A.Y.T. Leung, J.K.W. Chan, Fourier p-element for the analysis of beams and plates, *Journal of Sound and Vibration* 212 (1998) 179–185.
[4] A.Y.T. Leung, B. Zhu, J.J. Zheng, H. Yang, Analytic trapezoidal Fourier p-element for vibrating plane problems, *Journal of Sound and Vibration* 271 (2004) 67–81.
[5] Y.K. Cheung, *Finite Strip Method in Structural Analysis*, Pergamon, Oxford, 1976.
[6] T.J.R. Hughes, E. Hinton, *Finite Element Methods for Plate and Shell Structures*, Vol. 2, Pineridge pr., Swansea, 1986.
[7] A.Y.T. Leung, *Dynamic Stiffness and Substructures*, Springer, London, 1993.
[8] D.J. Gorman, *Free Vibration Analysis of Rectangular Plates*, Elsevier, New York, 1982.
[9] A.W. Leissa, The free vibration of rectangular plates, *Journal of Sound and Vibration* 31 (1973) 257–293.
[10] G.K. Xiu, Y.C. Jia, *Vibration Engineering*, Machine Industry, Beijing, 1983.